

# Impact of the Usage of a Slotted Cathode Carbon Block on Thermoelectric Field in an Aluminum Reduction Cell

WENJU TAO,<sup>1,2</sup> TUOFU LI,<sup>1,2</sup> ZHAOWEN WANG,<sup>1,2,3</sup>  
BINGLIANG GAO,<sup>1,2</sup> ZHONGNING SHI,<sup>1,2</sup> XIANWEI HU,<sup>1,2</sup> and  
JIANZHONG CUI<sup>1</sup>

1.—School of Materials and Metallurgy, Northeastern University, Shenyang 110819, Liaoning, People's Republic of China. 2.—Key Laboratory of Ecological Utilization of Multi-Metal Intergrown Ores of Education, Northeastern University, Shenyang 110819, Liaoning, People's Republic of China. 3.—e-mail: wangzw@smm.neu.edu.cn

The horizontal current in a metal pad of an aluminum reduction cell is critical because of its effect on the fluctuation of the metal pad. In this study, a novel cathode with a slotted cathode carbon block was proposed to decrease the horizontal current. The effects of the slotted cathode carbon block on the horizontal and vertical currents in the metal pad, cathode voltage, and temperature distribution in the cathode were calculated using the finite-element method. The results show that the slotted cathode carbon has great potential to decrease the horizontal current. When the length of slot  $b$  equals 400 mm, the maximum horizontal current density decreased by 50.4%. However, the cathode voltage in the cathode with the slotted cathode carbon was ~43 mV higher than that in a conventional cell, and the temperature in the slotted cathode carbon was slightly higher than that in a conventional carbon cell. Moreover, with increasing length of slot  $b$ , the maximum horizontal and vertical currents in the metal pad moved toward the cell center. The result of this study may provide the database in understanding the effect of the slotted cathode carbon on cell.

Aluminum is produced by the Hall–Heroult electrolytic reduction process by electrolysis of dissolved alumina in a molten electrolyte. The Hall–Heroult reduction cell (aluminum reduction cell) is used for the production of aluminum in an industrial setting. Although the cell designs have undergone substantial improvements over the time, the design of modern aluminum reduction cells is still similar to the earliest cell designs. The cells are operated at low voltage (~4 V) and high currents (180–500 kA). The direct current enters the cell through the anode and passes through electrolyte (molten cryolite) and metal pad (molten aluminum) to the cathode carbon block. The current is carried out of the cell by cathode collector bars. Notably, the current flows through the least resistance. The current path to the surface of the cathode carbon block close to the side of the cell is much shorter than the path to the surface of the cathode carbon block close to the center of the cell, as shown in Fig. 1.

Because of the highly conductive metal pad, horizontal currents establish themselves in the metal pad. The horizontal current and vertical magnetic field generate vortices and produce stirring in the metal pad,<sup>1</sup> which have adverse effects on the cell current efficiency and energy consumption. Furman<sup>2</sup> pointed out that the horizontal current was affected by the structure of the cell. Therefore, some cell designs have been proposed to decrease the horizontal current by changing the basic design of the cathode collector bar. Hudson et al.<sup>3</sup> and McGeer<sup>4</sup> proposed that using many more collector bars, the connector bar comprised a lighter gauge material to carry the current from the collector bar to the bus system. However, this design failed in practical applications because of the necessity of preassembling cathode carbon on the collector bars, and the lighter gauge connector bars were too weak to be handled safely by workers or cranes during the maintenance operations, thus requiring heavy labor for smelters. Moreover, the

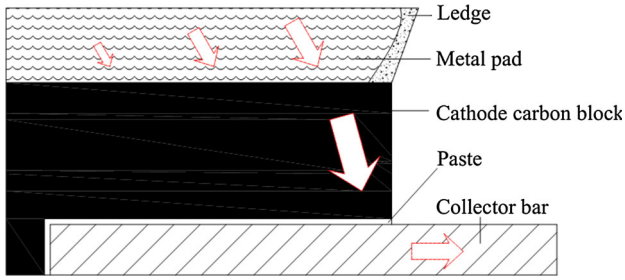


Fig. 1. The current path in cathode system.

design needs lots of changes in the conventional cathode bars and current bus, requiring major capital investment. Townsend<sup>5</sup> and Yang<sup>6</sup> put forward a type of slotted collector bar, acting as an insulator because the electrical resistance of refractory cement is much higher than that of a cathode collector bar. However, the temperature in a cathode with slotted collector bars is higher than that in a cathode with a conventional cathode collector.<sup>7</sup> The electrolyte intruding in the cathode carbon will be in a liquid state if the temperature is higher than the liquidus temperature of the electrolyte, and the collector bar will be eroded by the liquid electrolyte, decreasing the cell life.

Some researchers have attempted to equalize the current flow by changing the shape of the cathode carbon block or modifying it with different resistivities. Feng<sup>8</sup> designed an inclined cathode carbon block, similar to the cathode carbon block used in a drained cell. However, many problems, such as cathode carbon erosion, short cathode life,<sup>9</sup> and increased tendency to sludge formation,<sup>10</sup> linked with the inclined cathode carbon about drained cells have been reported. Winttner<sup>11</sup> tried to arrange the carbon block with a higher resistivity near the side of the cell. Unfortunately, the carbon block with a high resistivity will turn to lower resistivity block at higher temperatures. Therefore, using different carbon blocks does not provide the expected results.

The designs mentioned in the literature often are not economically feasible because they require either major capital investment or a lower life time of the cell. In this study, a novel cathode structure with the slotted cathode carbon block was proposed to decrease the horizontal current. The effect of the slotted cathode carbon block on the horizontal current was calculated using the finite-element method. Moreover, because of the high current and Joule heat in the cathode, it was vital to acquire more knowledge about the thermoelectric distributions in the cathode with the slotted cathode carbon. The effects of the slotted cathode carbon on the cathode voltage and temperature distribution in the cathode carbon block were also investigated.

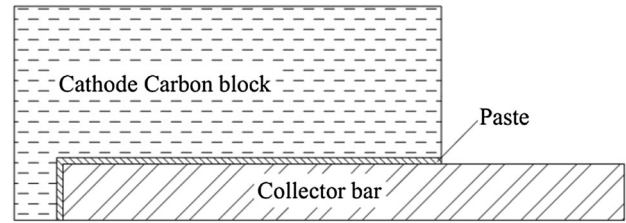


Fig. 2. Schematic diagram of conventional cathode structure.

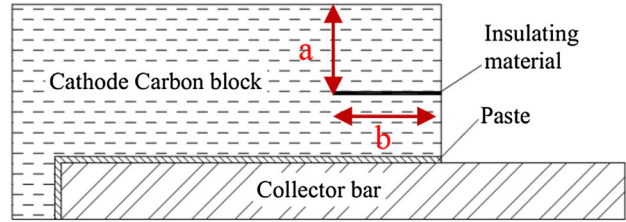


Fig. 3. Schematic diagram of a novel cathode structure with a slotted cathode carbon block.

## NOVEL CATHODE STRUCTURE WITH SLOTTED CATHODE CARBON BLOCK

Figure 2 shows the schematic diagram of a conventional cathode structure, comprising a cathode carbon block, paste, and collector bar. Figure 3 shows a novel cathode structure with a slotted cathode carbon block. The slot formed in the cathode carbon block is filled with an insulating material by an appropriate method.

Figure 4 shows the graphical depiction of the current paths. Figure 4a clearly shows that the closer the carbon block is to the external bus, more currents will pass through the carbon block. The slot filled with an insulating material is used to equalize the current flow in the carbon block.

## THERMOELECTRIC THEORY AND MODEL

### Governing Equations

The governing equations for the heat transfer and electrical potential distribution are:<sup>12</sup>

$$\frac{\partial}{\partial x}(\lambda_x \frac{\partial T}{\partial x}) + \frac{\partial}{\partial y}(\lambda_y \frac{\partial T}{\partial y}) + \frac{\partial}{\partial z}(\lambda_z \frac{\partial T}{\partial z}) + q = 0 \quad (1)$$

$$\nabla[\sigma \nabla V] = 0 \quad (2)$$

where  $T$  is temperature,  $\lambda$  is the thermal conductivity,  $\sigma$  is the electrical conductivity,  $V$  is the electrical potential, and  $q$  is the heat generation rate per unit volume (Joule effect). For a small volume, when the current flows, the Joule heat per unit volume is given by the following equation:

$$q = \sigma \times (-\nabla V)^2 \quad (3)$$

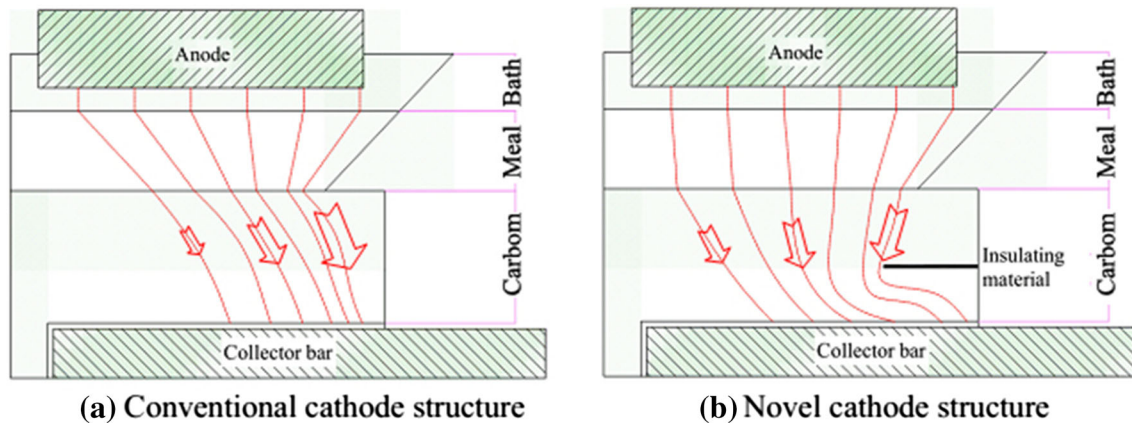


Fig. 4. The graphical depiction of current paths.

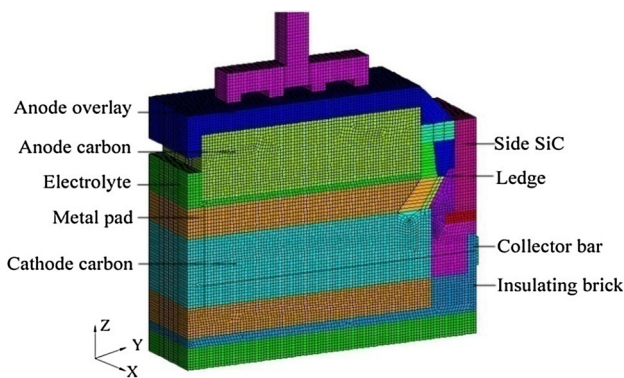


Fig. 5. The mesh of the thermoelectric model.

### Thermoelectric Coupled Model

A three-dimensional (3D) model is necessary to analyze the thermoelectric field. Because of the symmetry of the cell, only half of the geometric model was built as a computational domain. Figure 5 shows the mesh of the thermoelectric model.

The commercial software ANSYS (Ansys Inc., Canonsburg, PA) was used for the coupled thermoelectric calculation. The total number of elements for the 3D model is 304,896. The thermoelectric coupled element SOLID69 was used to transmit heat and current as well as generate Joule heat. The thermal-only element SOLID70 was used to simulate the heat transfer for thermal insulating materials. CONTACT170 and TARGET173 were used to simulate the thermal contact.

### Boundary Conditions

#### Electrical

The end of the collector bar was at zero potential. On the top surface of the anode rod, constant current was entered at a constant floating potential.

This was achieved by coupling the voltage on the surface nodes, whereas constant forcing current was applied on one of its node.<sup>13</sup>

#### Thermal

The temperature of the electrolyte and metal pad was assumed to be uniform.

Heat losses from the shell surface to ambient air occurred by convection. Moreover, the convective heat-transfer coefficient between the melt and ledge was defined as the thermal contact conductance coefficient.<sup>14</sup>

One of the challenging problems in the model is the changing thickness of the ledge with temperature. Dupuis<sup>15</sup> and Cui et al.<sup>16</sup> used the ANSYS Parametric Design Language (APDL) to relocate the nodes on the surface of the freeze. Figure 6 shows the flowchart of the freeze profile algorithm.

## RESULTS AND DISCUSSION

### Current Distribution in the Metal Pad

The current distribution in the cell was calculated using the metal height, electrolyte height and the anode cathode distance of 20 cm, 19 cm, and 4 cm, respectively. All the calculations were performed for a 300-kA aluminum reduction cell.

In the model, the effects of the length of the slot on the current distribution in the metal pad were investigated as listed in Table I.

In Table I, case 1 is the base case (Conventional cathode structure),  $a$  is the distance from the slot to the upper surface of the carbon block, and  $b$  is the length of slot.

Figure 7 shows the vector plot of the current density in the metal pad, indicating that the vector plots of the current density in the metal pad significantly changed in the cell with the slotted cathode carbon block. The maximum current density in the conventional cell is located in the ledge toe position. With increasing length of slot  $b$ , the

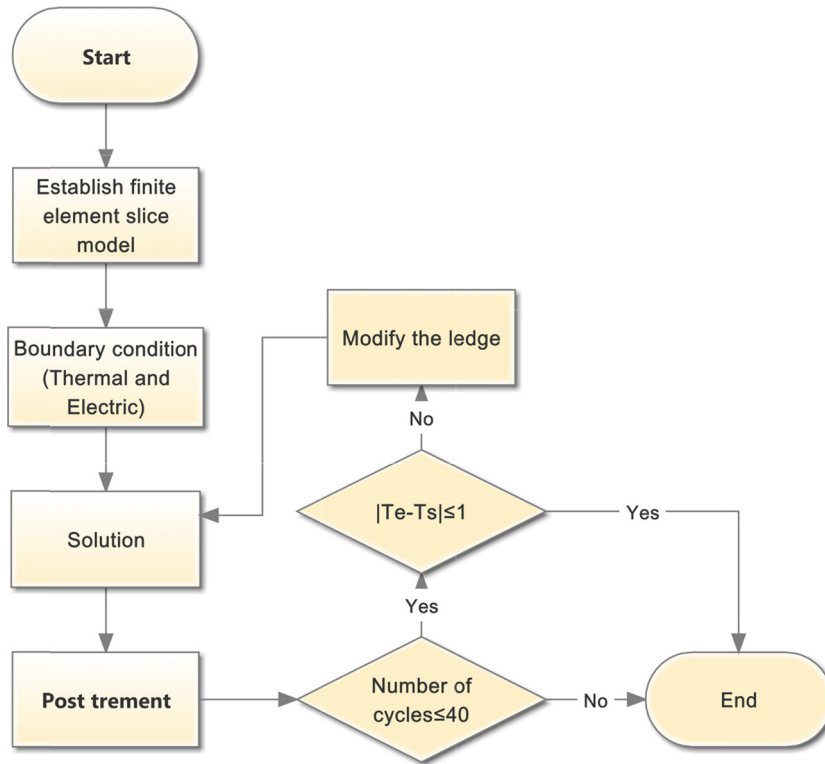


Fig. 6. Flow chart of the freeze profile algorithm.

**Table I. Four cases with various slotted cathode carbon blocks**

Case no.	$a$ (mm)	$b$ (mm)
1	0	0
2	150	200
3	150	300
4	150	400

maximum current density shifts from the ledge toe position toward the cell center.

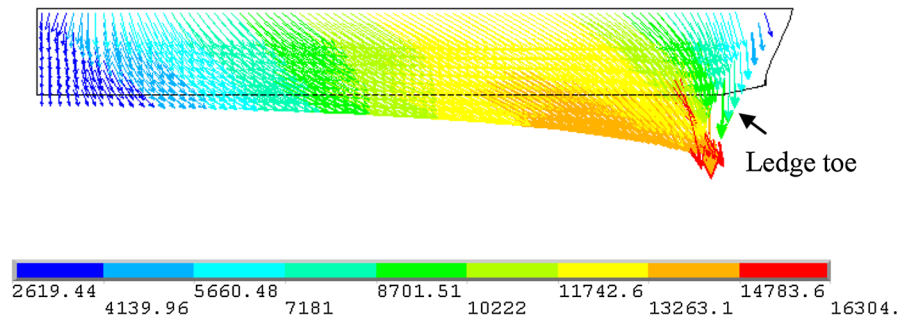
Figure 8 shows the effect of different length of slot  $b$  on the current distribution at the lower surface of the metal pad, clearly indicating that the current distribution in case 1 gradually increases to a maximum value. However, the current distribution in cases 2–4 gradually increases to a maximum value, then rapidly decreases to a minimum value.

Figure 9 shows the effects of different lengths of the slot on the current distribution at the upper surface of the metal pad. It is found that the varying tendencies of current density at the upper surface of the metal are similar and all gradually increase to a maximum value and then decrease to a minimum value. Clearly, with increasing length of slot  $b$ , the peak of the current density (the maximum current density) decreases and shifts toward the cell center.

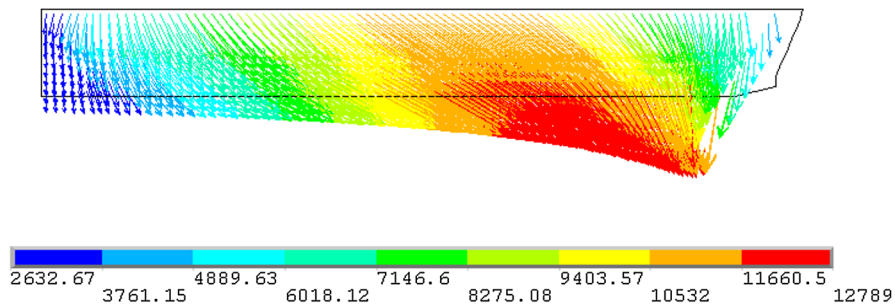
Figure 10 shows the vertical current distribution at the lower surface of the metal pad. Notably, the vertical current at the lower surface of the metal pad shows the current through the metal pad to the cathode carbon block. In case 1, the closer the metal pad to the ledge toe, the more vertical is the current through the metal pad into the cathode carbon block. This is an important reason for generating the horizontal current in the metal pad. Compared with case 1, the vertical current distributions at the lower surface of the metal pad significantly changed in cases 2–4. With increasing length of the slot  $b$ , the maximum vertical current density shifts from the ledge toe position toward the cell center, allowing more current to pass through the metal pad located near the cell center into the cathode carbon block.

The horizontal current distribution and the maximum horizontal current density at the upper surface of the metal pad are shown in Figs. 11 and 12, respectively. Figure 11 shows that the slotted cathode carbon significantly affects the horizontal current and greatly decreases. Figure 12 shows that when the length of the slot equals 400 mm (case 4), the maximum horizontal current decreases from  $11,120 \text{ A m}^{-2}$  to  $5517 \text{ A m}^{-2}$  (50.4%). Moreover, when the length of slot  $b$  increases, the peak of the horizontal current density shifts toward the cell center (Fig. 11).

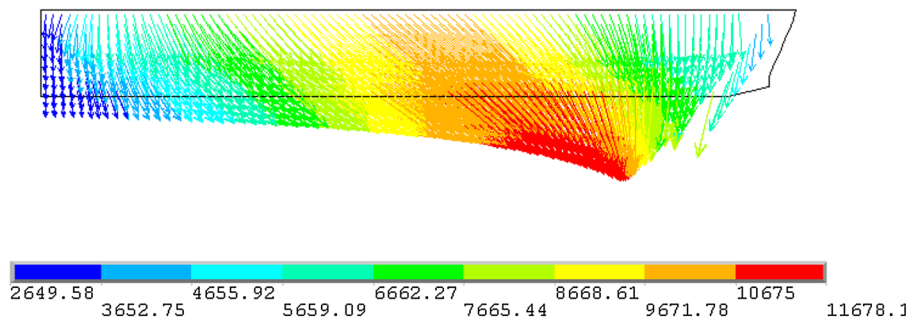
Case1



Case2



Case3



Case4

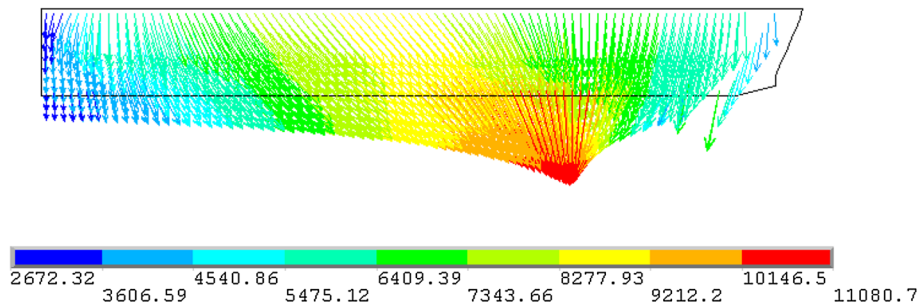


Fig. 7. Vector plot of current density in the metal pad in  $A/m^2$ .

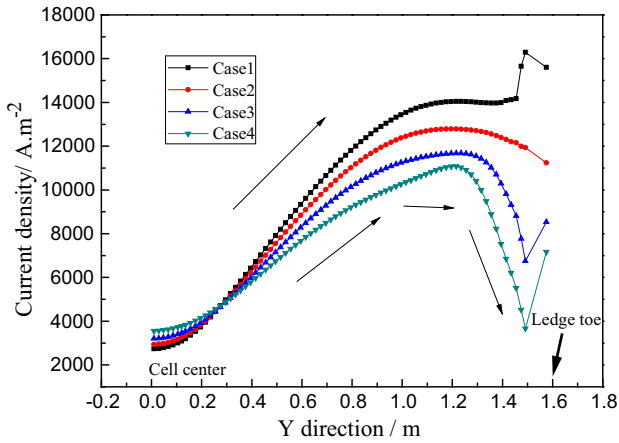


Fig. 8. Current distribution at the lower surface of the metal pad.

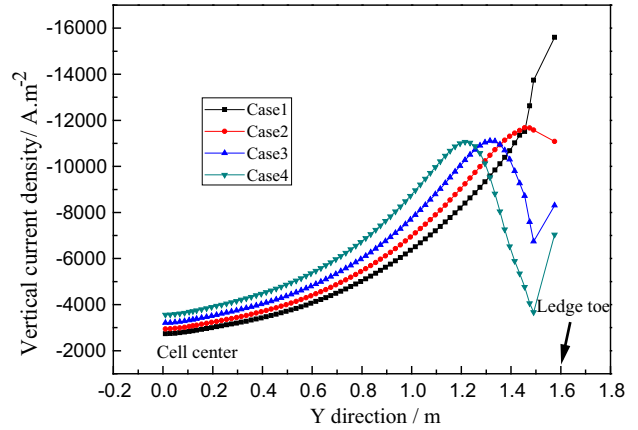


Fig. 10. Vertical current distribution at the lower surface of metal pad.

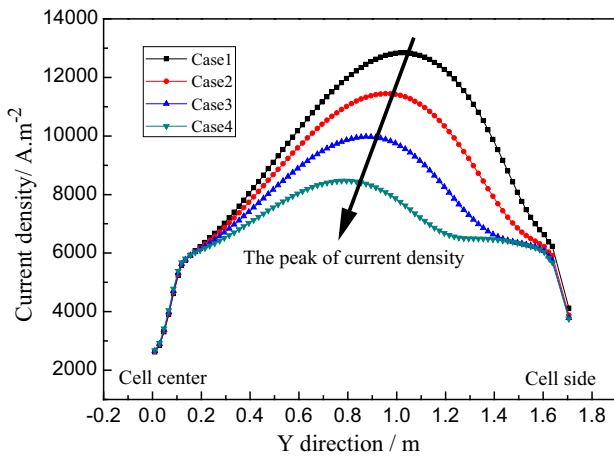


Fig. 9. Current distribution at the upper surface of the metal pad.

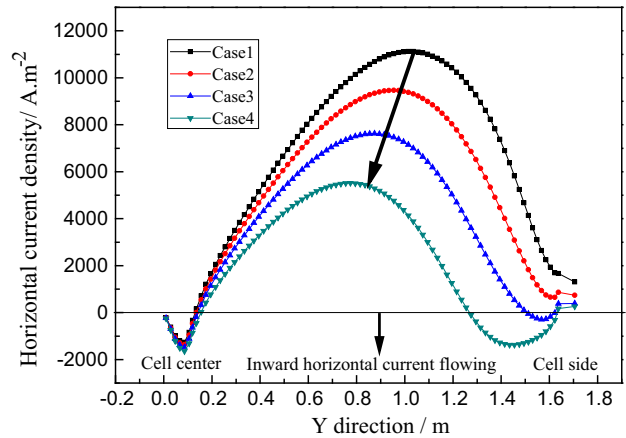


Fig. 11. Horizontal current distribution at the upper surface of the metal pad.

The above-mentioned results show that the slotted cathode carbon block has a significant effect on the horizontal and vertical current distribution in the metal pad. The horizontal current can be significantly decreased.

### Voltage Drop and Temperature Distribution in the Cathode

The voltage drop is an important parameter for the energy consumption of the cell. The slot in the cathode carbon block changes the structure of the cathode circuit and cathode voltage. Figure 13 shows the contour map of the cathode voltage clearly indicating that the cathode voltage drop in the novel cell is higher than that in the conventional cell. The cathode voltage will increase with increasing the length of slot *b*. When the length of slot *b* was 400 mm (in Case4), the cathode voltage increased by 43 mV.

Figure 14 shows the contour map of the temperature in the cathode carbon block and Fig. 15

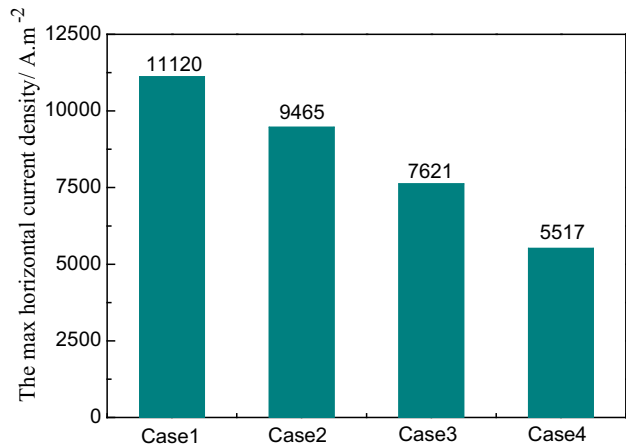
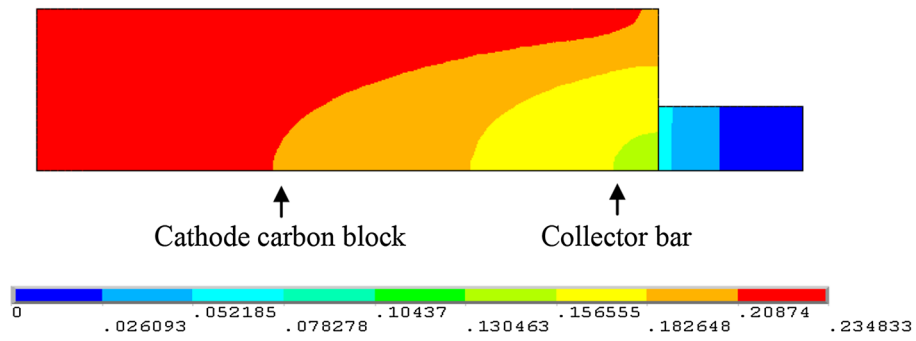


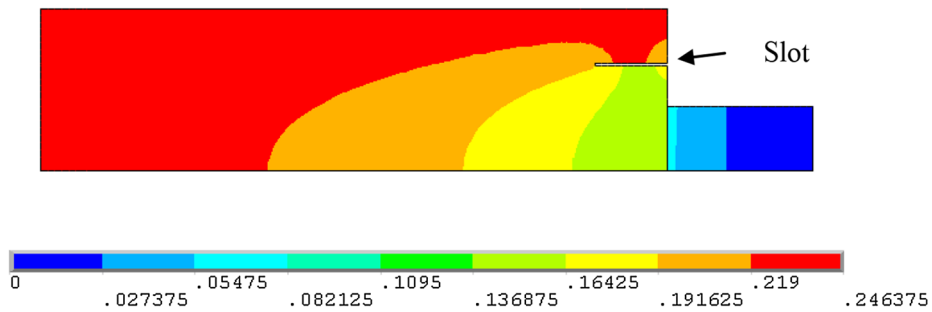
Fig. 12. Maximum horizontal current density at the upper surface of the metal pad.

represents the temperature distribution at the bottom of the cathode carbon block. These curves show that the slot has a slight effect on the

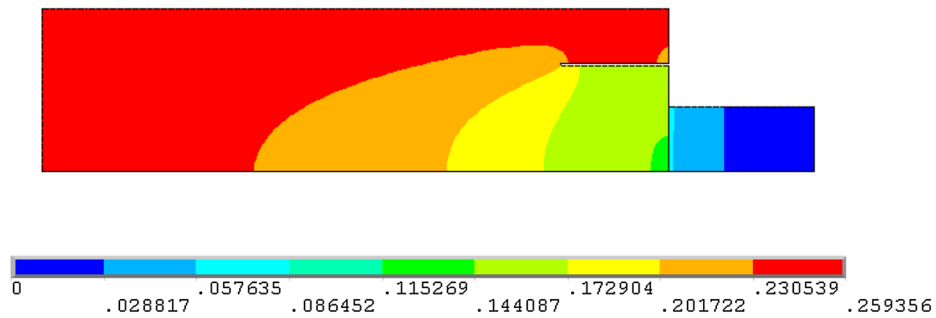
Case 1



Case 2



Case 3



Case 4

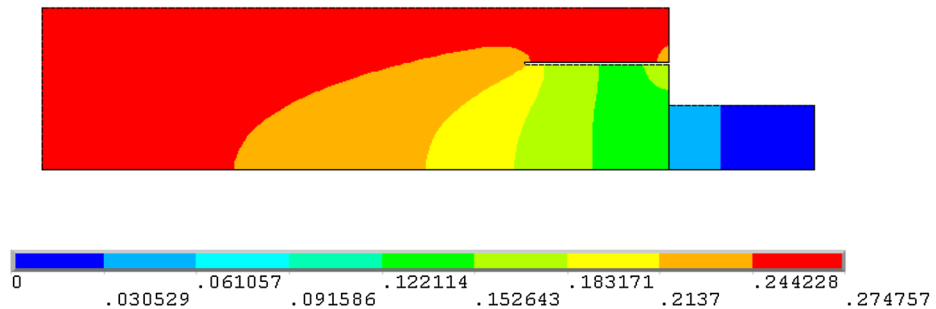


Fig. 13. Contour map of cathode voltage (V).

temperature distribution in the cathode carbon block. Although the temperature in the slotted cathode carbon block is higher than that in a conventional cathode carbon block, the temperature difference is very small.

### CONCLUSION

The horizontal current in the metal pad of an aluminum reduction cell is critical because of its effect on the cell current efficiency and energy

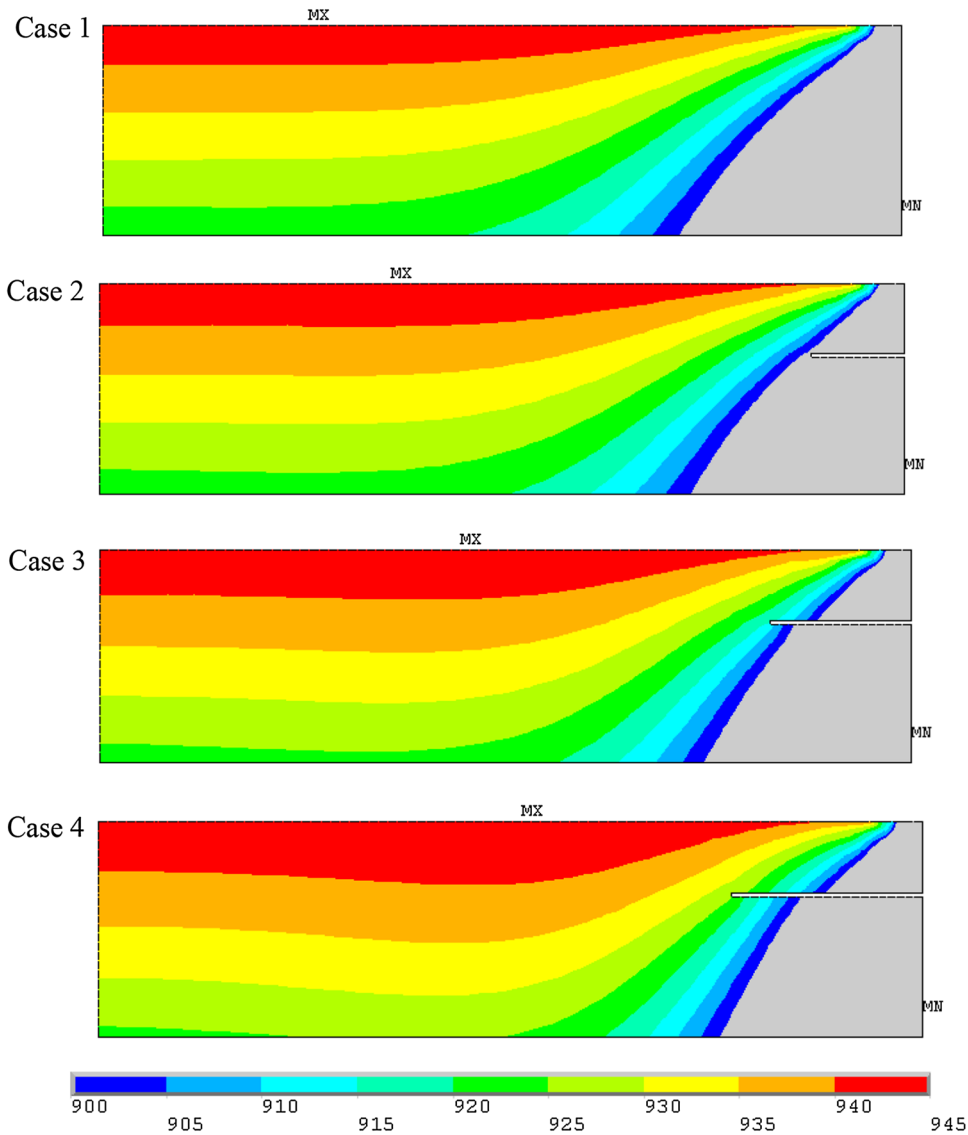


Fig. 14. Contour map of temperature in cathode carbon block (°C).

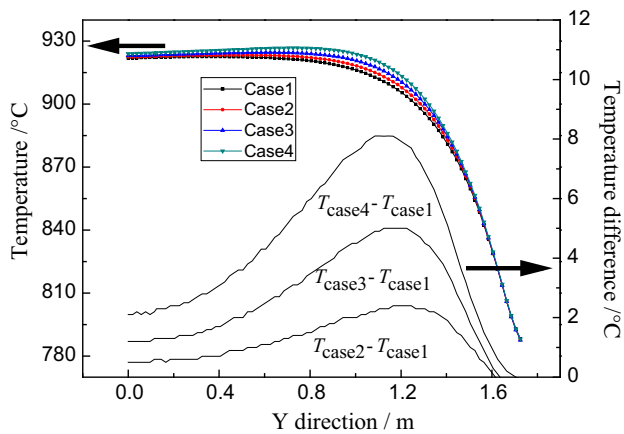


Fig. 15. Temperature distribution at the bottom of the cathode carbon block.

consumption. In this study, a novel cathode structure with a slotted cathode carbon block was proposed to decrease the horizontal current. The effects of this slotted cathode carbon block on the horizontal and vertical current in the metal pad, cathode voltage, and temperature distribution in the cathode were calculated using the finite-element method. The conclusions of this study are as follows:

1. The slotted cathode carbon block significantly affects the current distribution, particularly the horizontal current. With increasing length of slot  $b$ , the maximum horizontal and vertical currents moved toward the cell center, and the horizontal current at the upper surface of the metal pad is significantly decreased. When the length of the slot was 400 mm, the maximum horizontal current density decreased by 50.4%.



2. The cathode voltage drop will increase with increasing length of the slot  $b$ . When the length of slot  $b$  was to 400 mm, the cathode voltage increased by 43 mV. The slotted cathode carbon block has a slight effect on the temperature distribution in the cathode carbon block. Although the temperature in the slotted cathode carbon block is higher than that in a conventional cathode carbon block, the temperature difference is very small.

### ACKNOWLEDGEMENTS

The authors would like to express their gratitude for the financial support by the National Key Technology Research and Development Program of the Ministry of Science and Technology of China (Grant No. 2012BAE08B01), the National Natural Science Foundation of China (Grant Nos. 51228401, and 51322406, 51434005).

### REFERENCES

1. P.A. Davidson and R.I. Lindsay, *J. Fluid Mech.* 362, 327 (1998).

2. A. Furman, *Light Metals 1978*, ed. J.J. Miller (Warrendale, PA: TMS, 1978), pp. 87–106.  
3. T. Hudson, J. Huni, V. Potocnik, and D. MacMillan, U.S. patent 4,194,959 (1980).  
4. J. McGeer, U.S. patent 4,592,820 (1986).  
5. D. Townsend, U.S. patent, 4,795,540 (1989).  
6. S. Yang Al and Mg Eng. Res. Inst., China patent CN102453927A (2012) (in Chinese).  
7. C.G. Yin, J. Li, Y.J. Xu, S. Yang, Y.Q. Lai, N. Jiang, and H.L. Zhang, *Chin. J. Nonferr. Met.* 24, 246 (2014).  
8. N.X. Feng, China patent CN201110385777.0 (2012) (in Chinese).  
9. M.L. Walker, *Light Metals 1997*, ed. R. Huglen (Warrendale, PA: TMS, 1997), pp. 215–219.  
10. M.P. Taylor, W.D. Zhang, and V. Wills, *Chem. Eng. Res. Des.* 74, 913 (1996).  
11. H. Wintter and K. Lauer, U.S. patent 3,787,311 (1974).  
12. M. Blais, M. Desilets, and M. Lacroix, *Appl. Therm. Eng.* 58, 439 (2013).  
13. D. Richard, M. Fafard, R. Lacroix, P. Clery, and Y. Maltais, *Finite Elem. Anal. Des.* 37, 287 (2001).  
14. W.J. Tao, L. Wang, Z.W. Wang, B.L. Gao, Z.N. Shi, X.W. Hu, and J.Z. Cui, *JOM* 67, 322 (2015).  
15. M. Dupuis, *Light Metals 1998*, ed. B.J. Welch (Warrendale, PA: TMS, 1998), pp. 409–418.  
16. X.F. Cui, H.L. Zhang, Z. Zou, J. Li, Y.Q. Lai, Y.J. Xu, H.H. Zhang, and X.J. Lv, *Light Metals 2010*, ed. J.A. Johnson (Warrendale, PA: TMS, 2010), pp. 447–452.